VALIDATING FE HYBRID III, THOR, AND GHBMC M50-OS FOR FUTURE SPACEFLIGHT CONFIGURATION TESTING

Kyle P. McNamara[1,2], Derek A. Jones[1,2], James P. Gaewsky[1,2], Xin Ye[1,2], Bharath Koya[1,2], Mona Saffarzadeh[1,2], F. Scott Gayzik[1,2], Ashley A. Weaver[1,2], Joel D. Stitzel[1,2]
[1]Wake Forest School of Medicine, [2]Virginia Tech-Wake Forest University Center for Injury Biomechanics

ABSTRACT

Between 1976 and 2013, a combination of Hybrid III, THOR, and human volunteer tests were conducted using both the Horizontal Impulse Accelerator (HIA) and Vertical Deceleration Tower (VDT) at Wright-Patterson Air Force Base and USAF Armstrong. These tests formed a matrix for finite element (FE) validation. This study analyzes a physical test configuration with accelerations in the frontal (X-) direction. The acceleration magnitude was 10 G with a pulse duration of 70 ms. Simulations were performed using the Humanetics 50th percentile male Hybrid III, NHTSA THOR 50th male, and the Global Human Body Models Consortium (GHBMC) 50th male simplified occupant (M50-OS) FE models in LS_DYNA. All simulations consisted of a 150 ms period of gravitational settling and belt pretensioning followed by the acceleration pulse taken from the physical test of interest. Analysis consisted of both a visual comparison of kinematics as well as a quantitative analysis. Simulation acceleration signals in the head, neck, thorax, and pelvis as well as belt forces were compared to matched physical signals using the Gehre et al. method (CORrelation and Analysis, or CORA, size phase, and shape). Visual inspection for the test configuration simulations showed agreement with the physical test cases in regards to the excursion magnitude and direction of the thorax and the head. The CORA scores for the three simulations ranged from 0.613 to 0.908 on a scale from 0 to 1, with 1 being a perfect score.

INTRODUCTION

The overall purpose of this study is to understand the extent to which 50th percentile male anthropomorphic test devices (ATDs) predict injury risks in spaceflight-like loading conditions. Injury assessment reference values (IARVs) currently in use were generated from data which employed post-mortem human subjects postured in specific configurations to determine injury risks to occupants. Primarily, these tests were conducted in both automotive and military research, and may not translate directly to spaceflight. Namely, there are differences in the loading directions, postures, and restraint systems in spaceflight.

This study begins to addresses these differences by validating finite element (FE) models of ATDs and FE human body models (HBMs) against physical dummies and human volunteers in frontal loading directions. This step is crucial for future spaceflight seat design, in which the occupants are subjected to various loading directions and magnitudes.

METHODS

Data Source

Hybrid III, THOR, and human volunteer tests were performed using both the Horizontal Impulse Accelerator (HIA) and Vertical Deceleration Tower (VDT) at Wright-Patterson Air Force Base and USAF Armstrong Laboratory (Hearnon and Brinklet 1986, Buhrman and Perry 1994, Perry, Burneka et al. 2013). All ATD and human tests used either a 4-point or 5-point belt restraint system in a flat pan seat with a vertical back (Perry, Burneka et al. 2013). A total of 273 tests were performed comprising 35 Hybrid III, 26 THOR, and 212 human male volunteer physical tests with accelerations in the frontal (X-), rear (X+), lateral (Y), and vertical (Z+) directions. From these tests, the frontal (X-) 10 G impact with a 70 ms rise time performed for Hybrid III, THOR, and human volunteers was selected for initial validation.

Video Review

A thorough review of video recordings from the impacts was conducted in order to identify test conditions, seat configurations, belt parameters, and body kinematics during physical impact (Figure 1). This was performed in order to better replicate the physical data in simulations. We looked for instances that deviated from the desired testing conditions such as arms/legs flying off their straps. Documentation of body kinematics included head rotation/flexion, neck extension, thorax moving to left/right, head hitting the side plates/head rest, hands/feet remaining strapped, arms/legs flying off the strap, hands/legs hitting the side plates, hands/legs extension and feet dorsiflexion. While ATD video quality was sufficient, the quality of video captured in the human volunteer tests varied based on year of test (1976-2003) and thus dictated the ability to accurately capture the above observational measures. When possible, each observation was recorded.

(a) (b)

Figure 1: Video still frames from - X, 10G, 70ms rise Hybrid III test. These figures represent the starting position (a) and maximum excursion (b) during the physical test.

Acceleration Pulse Creation

Crash pulse signals were extracted from MATLAB files in the test documentation and categorized based on their directionality, rise time to reach peak acceleration, and magnitude of peak acceleration. The variable "pulse duration" was included in physical test data and represented the time at which the acceleration pulse had returned to approximately zero, after the half-sine wave. This value was increased by 20% to dictate the portion of the sled pulse that was fed into the FE simulations (see below). Thus, each simulation was conducted to 120% of the duration of the crash pulse phase. In the case of multiple physical tests in a given configuration, the larger "pulse duration" value was used.

FE Simulations

Simulations of the three frontal (-X), 10G, 70ms rise time Hybrid III, THOR, and human volunteer physical tests were performed using the Humanetics 50th percentile male Hybrid III, National Highway Traffic Safety Administration (THOR) 50th male, and the Global Human Body Models Consortium (GHBMC) 50th male simplified occupant (M50-OS) FE models in LS_DYNA (MPP, Version 971, R 6.1.1, LSTC, Livermore, CA) on the Wake Forest University DEAC cluster (2012, Panzer, Giudice et al. 2015, Schwartz, Guleyupoglu et al. 2015). Prior to activation of the crash pulse, a 150ms gravitational settling period was applied to the FE models. This period allowed for proper positioning of the models into the seat configurations. A visual inspection was performed to ensure that the models matched the testing configuration postures seen in the videos from physicals tests.

The simulation belts were pre-tensioned during the 150ms settling period using a peak pretensioner force averaged from the test data. Immediately before applying the acceleration pulse to the seat frame, the seat belt retractors were locked. This was done to model the physical testing which did not allow payout of the belt system.

In order to better replicate spaceflight occupant kinematics, multiple boundary conditions were assigned to the model. These included assigning both hands of the GHBMC model to move along with the femurs. A foot strap noted in physical testing led to the constraining of the ankles to the seat. Rotational movement of the seat was prevented throughout the whole simulation. During the crash pulse, translational seat movement was moved only along the direction of the applied crash pulse.

In the –X, 10G, 70ms rise time simulations, two types of restraint systems were used in physical testing: the PCU-16/P harness and lap belt combination and the MB-6 belt system. The PCU-16/P torso harness is a single-unit assembly that covers individuals below the 5^{th} percentile range. In modeling this harness, a chest strap, lower back strap, and two loops around the upper thighs were included, while the crossing back straps were excluded. The lap belt, which was included in the physical testing but was not attached to the PCU-15/P harness was also modeled. The MB-6 belt consisted of a conventional restraint system of double shoulder belts and lap belt (Figure 1). A negative-G crotch belt was used for Hybrid III and THOR simulations, but was not present in video review of human testing and therefore not modeled during the human

simulations. All belts were modeled as a combination of 2D shell elements and 1D seatbelt elements that were anchored to the chairs. Where webbing was attached with buckles, constrained nodal rigid bodies (CNRBs) were modeled.

Data Analysis

Simulation acceleration signals in the head, neck, thorax, and pelvis as well as belt forces were compared to matched physical signals using the Gehre et al. method (CORrelation and Analysis, or CORA, size, phase, and shape) (Gehre, Gades et al. 2009). This method compared simulation results against their matched physical test results to determine an overall ranking of the quality of the signal (Figure 2). The ability of the simulation signal to match the phase, shape, and magnitude of the average physical results was independently determined. An average of these scores composed a cross correlation method score. All scores were assessed on a 0 to 1 scale, with 1 denoting a perfect score.

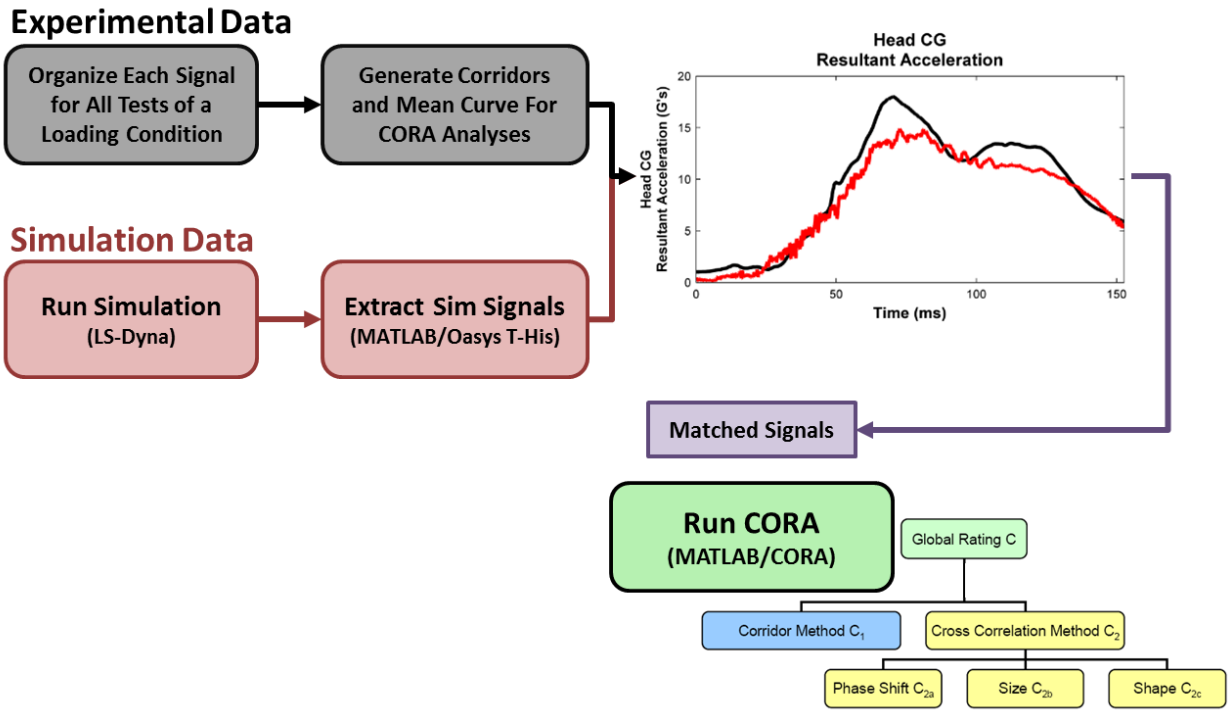

Figure 2: CORA score calculation algorithm compares the overall quality of simulation signals in comparison to their matched physical signals to generate an overall score from 0 to 1, with 1 denoting a perfect score.

In the Hybrid III impact, CORA scores were generated for the resultant accelerations of the head CG, chest (measured at vertebra T6), and pelvis. CORA scores were also generated for the resultant forces in the left and right shoulder and lap belts as well as the middle crotch belt. These CORA scores were weighted to generate an overall rating of the simulation (Equation 1).

$$C_{Total\ Response} = \frac{1}{2}\sqrt{C_{Head}^2 + C_{T6}^2 + C_{Pelvis}^2 + \left(\frac{C_{L-Lap}+C_{R-Lap}+C_{L-Shoulder}+C_{R-Shoulder}+C_{Groin}}{5}\right)^2} \quad \textbf{Equation 1}$$

In the THOR impact, CORA scores were generated for the resultant accelerations of the head CG, chest (measured at vertebras T1 and T12), and pelvis. CORA scores were also generated for the resultant forces in the left and right shoulder and lap belts as well as the middle crotch belt. These CORA scores were weighted to generate an overall rating of the simulation (Equation 2).

$$C_{Total\ Response} = \frac{1}{\sqrt{5}}\sqrt{C_{Head}^2 + C_{T1}^2 + C_{T12}^2 + C_{Pelvis}^2 + \left(\frac{C_{L-Lap}+C_{R-Lap}+C_{L-Shoulder}+C_{R-Shoulder}+C_{Groin}}{5}\right)^2} \quad \textbf{Equation 2}$$

In the human/GHBMC impact, CORA scores were generated for the resultant accelerations of the head CG and chest. CORA scores were also generated for the resultant forces in the left and right shoulder and lap belts. These CORA scores were weighted to generate an overall rating of the simulation (Equation 3).

$$C_{Total\ Response} = \frac{1}{\sqrt{3}}\sqrt{C_{Head}^2 + C_{Chest}^2 + \left(\frac{C_{L-Lap}+C_{R-Lap}+C_{L-Shoulder}+C_{R-Shoulder}}{4}\right)^2} \quad \textbf{Equation 3}$$

RESULTS

The Hybrid III simulations show agreement of start and maximum excursion of the head and thorax with physical results (Figure 3). We do see persistent flexion of the elbows instead of the elbow extension seen in physical results. As seen in Figure 4, CORA scores for individual signals were high (0.886-0.974) with the exception of the middle crotch belt resultant force (0.619) which exhibited a higher magnitude than that measured physically. Overall rating of the simulation was high (0.908).

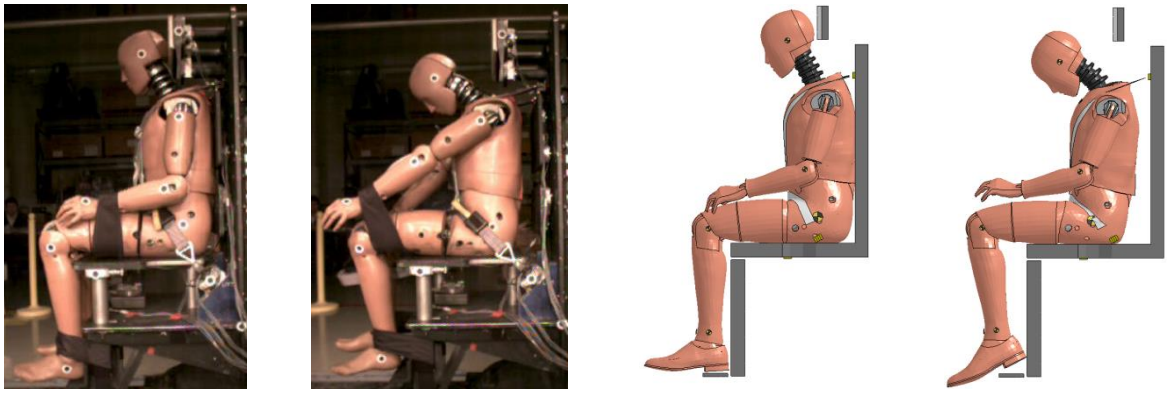

(a) (b) (c) (d)

Figure 3: Physical (a,b) and simulation (c,d) results of -X, 10G, 70ms rise Hybrid III test. Starting position (a,c) and maximum excursion (b,d).

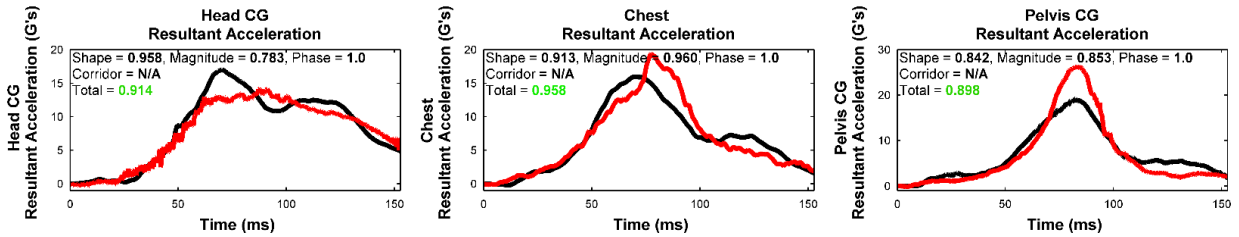

Figure 4: Physical (black) and simulation (red) signal analysis, including individual CORA and Overall scores for -X, 10G, 70ms rise Hybrid III test.

Qualitative analysis of the THOR simulations shows agreement of start and maximum excursion of the head and thorax compared with physical results (Figure 5). At maximum excursion, the simulation elbows remain flexed in contrast to the elbow extension seen in physical results. As seen in Figure 6, CORA scores for individual signals were high (0.652-0.953) with the lowest scores occurring in the lap belts and crotch belt (0.652-0.703). The low scoring signals exhibited low magnitude agreement with the physical data. Overall rating of the simulation was high (0.891).

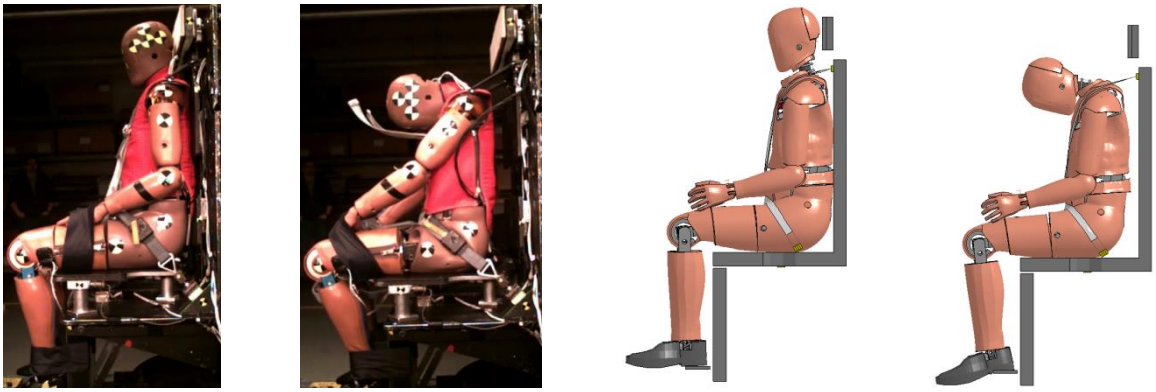

(a) (b) (c) (d)

Figure 5: Physical (a,b) and simulation (c,d) results of -X, 10G, 70ms rise THOR test. Starting position (a,c) and maximum excursion (b,d).

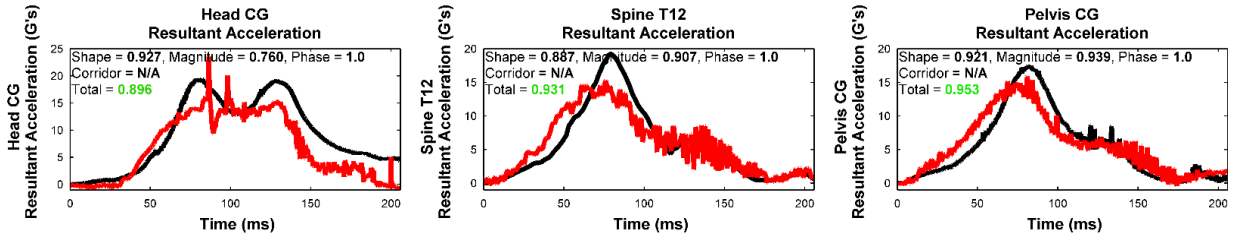

Figure 6: Physical (black) and simulation (red) signal analysis, including individual CORA and Overall scores for -X, 10G, 70ms rise THOR test.

Qualitative analysis of the GHBMC M50-OS simulations shows agreement of start and maximum excursion of the head, but increased thorax excursion compared with physical results (Figure 7). At maximum excursion, the simulation elbows remain flexed in contrast to the elbow extension seen in physical results. Overall excursions of the simulation were higher than the

physical test. As seen in Figure 8, CORA scores for individual signals were high (0.738-0.877) with the exception of the head CG acceleration (0.522) and the chest sternum X acceleration (0.456). Human tests did not include pelvis data and this belt configuration did not include a middle crotch belt. The low scoring signals exhibited low phase agreement with the physical data. Overall rating of the simulation was 0.613.

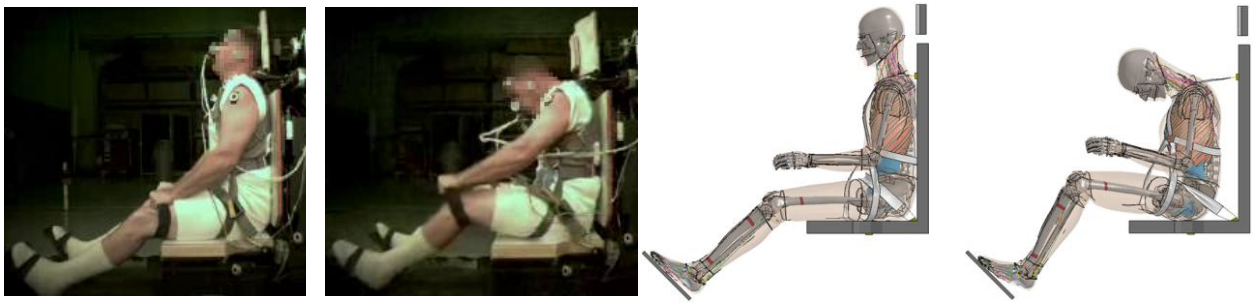

(a) (b) (c) (d)

Figure 7: Physical (a,b) and simulation (c,d) results of -X, 10G, 70ms rise human test. Starting position (a,c) and maximum excursion (b,d).

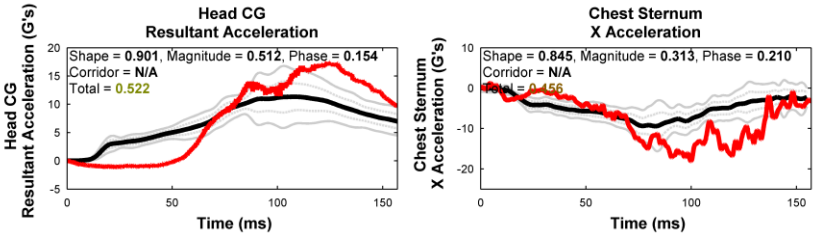

Figure 8: Physical (black) and simulation (red) signal analysis, including individual CORA and Overall scores for -X, 10G, 70ms rise human test. Corridors (gray) in the figure designate one standard deviation for the tighter corridor and two standard deviations for the wider corridor.

DISCUSSION

Overall, visual inspection of the frontal (X-), 10 G, 70ms test configuration simulation showed agreement with the physical tests for the Hybrid III, THOR, and human in regards to excursion magnitude and direction of the thorax and head. Persistent flexion of elbows at maximum excursion instead of extension in the simulations was noted. However, this does not affect the accelerations or maximum excursion of the chest. Simulation signals showed high levels of agreement with the exception of head CG resultant acceleration and chest sternum X acceleration in the human/GHBMC simulations. This is perhaps due to the variability in human volunteer responses and bracing during physical testing. Further variation in the maximum excursion of the thorax may be explained by the performance of the belting system. This suggests further opportunities for improving the GHBMC simulation.

CONCLUSIONS

Initial validation of ATD and human body models against physical test data is essential for building confidence in future applications of said models. Overall the physical and simulation results were comparable, ensuring confidence in FE model performance in the validated regime. The results of this study are highly applicable to both government and commercial spaceflight and provide confidence in FE simulation for future design. Future directions will include simulations to match the remaining test configurations and validate the entire regime.

ACKNOWLEDGEMENTS

This study was funded by NASA Human Health and Performance Contract (HHPC) through KBRWyle. Views expressed are those of the authors and do not represent the views of NASA or KBRwyle. Simulations were performed on the Wake Forest University DEAC cluster, a centrally managed resource with support provided in part by the university

REFERENCES

(2012). H350 Adult Dummy Model LS-Dyna. I. Humanetics Innovative Solutions.

Buhrman, J. R. and C. E. Perry (1994). "Human and manikin head/neck response to+ Gz acceleration when encumbered by helmets of various weights." Aviation, space, and environmental medicine **65**: 1086-1090.

Gehre, C., H. Gades and P. Wernicke (2009). Objective rating of signals using test and simulation responses. 21st International Technical Conference on the Enhanced Safety of Vehicles Conference (ESV). Stuttgart, Germany**:** 15-18.

Hearnon, B. F. and J. W. Brinklet (1986). "Effect of seat cushions on human response to+ Gz impact." Aviation, space, and environmental medicine **57**: 301-312.

Panzer, J. B., S. Giudice and J. B. Putnam (2015). THOR 50th male finite element model, User Manual, model v 2.1 for LS-Dyna. NHTSA/USDOT.

Perry, C., C. Burneka and C. Albery (2013). Biodynamic Assessment of the THOR-K Manikin, DTIC Document.

Schwartz, D., B. Guleyupoglu, B. Koya, J. D. Stitzel and F. S. Gayzik (2015). "Development of a computationally efficient full human body finite element model." Traffic Injury Prevention **16**(S49-S56).